CHEMISTRY OF MATERIALS
Cite This: Chem. Mater. 2018, 30, 2742−2749
Article
pubs.acs.org/cm

Ultrafast Electrochemical Expansion of Black Phosphorus toward High-Yield Synthesis of Few-Layer Phosphorene

Jing Li,[†,‡,¶] Cheng Chen,[†,¶] Shule Liu,[§] Junpeng Lu,[∥,⊥] Wei Peng Goh,[#] Hanyan Fang,[†] Zhizhan Qiu,[†,▽] Bingbing Tian,[†,‡] Zhongxin Chen,[†] Chuanhao Yao,[†,‡] Wei Liu,[†] Huan Yan,[†,‡] Ying Yu,[○] Dan Wang,[○] Yewu Wang,[○] Ming Lin,[#] Chenliang Su,*[,‡] and Jiong Lu*[,†,⊥]

[†]Department of Chemistry, National University of Singapore, 3 Science Drive 3, Singapore 117543

[‡]SZU-NUS Collaborative Center and International Collaborative Laboratory of 2D Materials for Optoelectronic Science & Technology, Engineering Technology Research Center for 2D Materials Information Functional Devices and Systems of Guangdong Province, College of Optoelectronic Engineering, Shenzhen University, Shen Zhen, 518060, China

[§]School of Materials Science and Engineering, Key Laboratory for Polymeric Composite and Functional Materials of Ministry of Education, Sun Yat-Sen University, Guangzhou 510275, P. R. China

[∥]Department of Physics, National University of Singapore, 2 Science Drive 3, Singapore 117542

[⊥]Centre for Advanced 2D Materials and Graphene Research Centre, National University of Singapore, 2 Science Drive 3, Singapore 117546

[#]Institute of Materials Research and Engineering, Agency for Science, Technology and Research (A*STAR), 2 Fusionopolis Way, Innovis, #08-03, Singapore 138634

[▽]NUS Graduate School for Integrative Sciences and Engineering, National University of Singapore, 28 Medical Drive, Singapore 117456

[○]Department of Physics & State Key Laboratory of Silicon Materials, Zhejiang University, Hangzhou 310027, P. R. China

Supporting Information

ABSTRACT: To bridge the gap between laboratory research and commercial applications, it is vital to develop scalable methods to produce large quantities of high-quality and solution-processable few-layer phosphorene (FLBP). Here, we report an ultrafast cathodic expansion (in minutes) of bulk black phosphorus in the nonaqueous electrolyte of tetraalkylammonium salts that allows for the high-yield (>80%) synthesis of nonoxidative few-layer BP flakes with high crystallinity in ambient conditions. Our detailed mechanistic studies reveal that cathodic intercalation and subsequent decomposition of solvated cations result in the ultrafast expansion of BP toward the high-yield production of FLBP. The FLBPs thus obtained show negligible structural deterioration, excellent electronic properties, great solution processability, and high air stability, which allows us to prepare stable BP inks (2 mg/mL) in low-boiling point solvents for large-area inkjet printing and fabrication of optoelectronic devices.

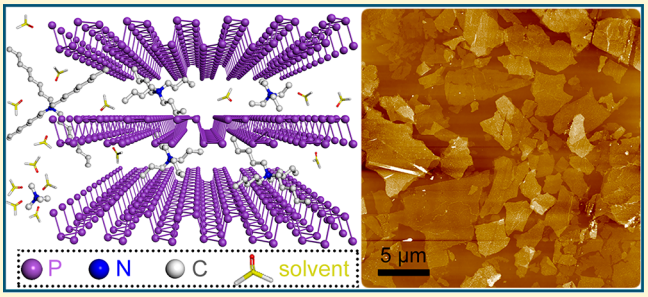

INTRODUCTION

Thin layers of black phosphorus (BP) have attracted great attention as next generation two-dimensional semiconductors due to their exceptional electronic,[1,2] photonic,[3−5] and in-plane anisotropic properties.[6−8] This new material possesses both high mobility and a layer-dependent direct bandgap spanning over a wide energy range from 0.3 eV for bulk BP to ∼2.0 eV for monolayer phosphorene,[9] which is unrivaled by any other 2D material known to date.[10] These properties are of great interest for potential applications in electronics and optoelectronics,[11,12] in particular for developing thin film transistors,[2] photodetectors,[3,13] ultrafast photonics,[14] flexible logic circuits, and sensors.[15] Similar to the field in graphene,[16] fully exploiting the properties of BP for real-life applications requires the mass production of high-quality few-layer phosphorene (FLBP) at a low cost. Unfortunately, FLBP notoriously exhibits environmental instability, which presents major hurdles in both its synthesis and processing.[17,18] Numerous attempts have been made for the production of FLBP thin flakes, including mechanical cleavage and solution-phase exfoliation.[7,11] Among the methods developed to date, mechanical cleavage has been the dominant technique employed at the laboratory-scale for the fabrication of electronic-grade FLBP flakes for device demonstration. However, the scope of this technique is limited

Received: February 3, 2018
Revised: April 2, 2018
Published: April 3, 2018

DOI: 10.1021/acs.chemmater.8b00521
Chem. Mater. 2018, 30, 2742−2749

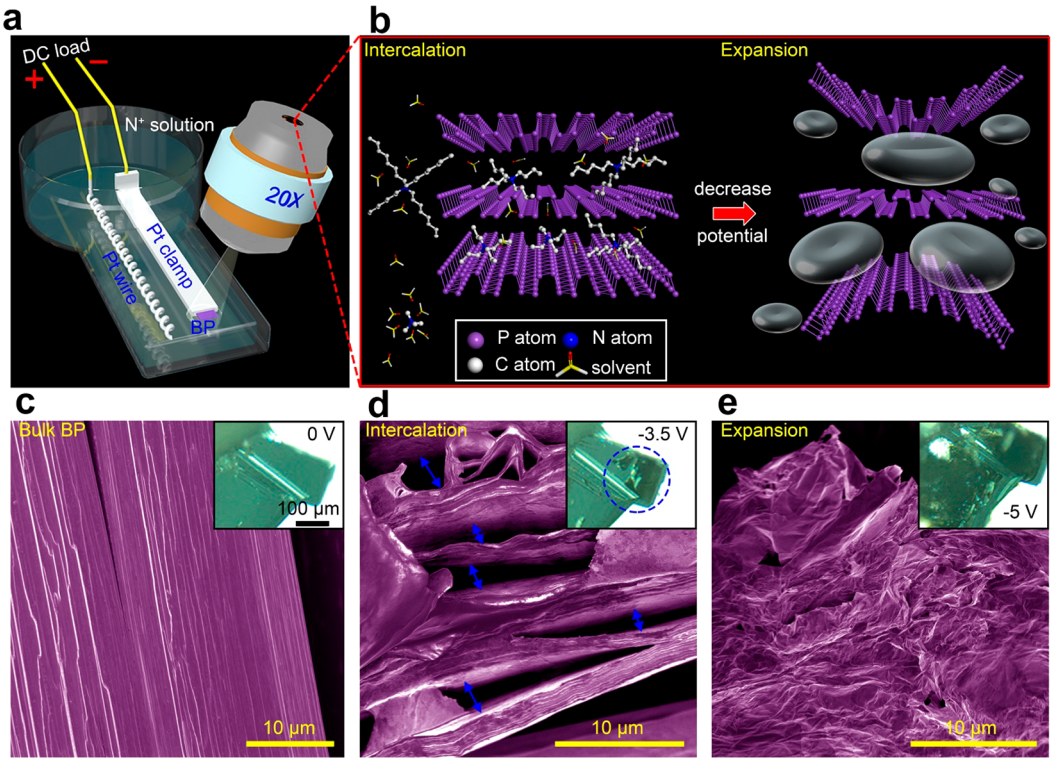

Figure 1. Electrochemical intercalation and expansion of bulk BP at the cathode. (a) Schematic illustration of a microelectrochemical cell mounted beneath an optical microscope. (b) Illustration of the intercalation and expansion of a BP cathode in organic DMSO electrolyte consisting of TAA salts. False color SEM imaging of the edge of bulk BP before and after applying different charging voltages ((c) 0 V; (d) −3.5 V; (e) −5 V). Double-arrows in d highlight the expansion gap between layered BP structures. Inset: the corresponding *in situ* optical microscopy imaging of bulk BP before and after applying different charging voltages. The dashed circle in the inset of d highlights the bumps formed on the BP surface.

due to a lack of scalability.[19] On the other hand, solution-phase exfoliation of bulk BP is considered as a facile and inexpensive method to produce BP nanosheets in large quantities. Unfortunately, this method generally involves prolonged agitation (ranging from several hours to days)[20,21] by sonication or shear mixing in inert atmosphere, inevitably leading to the production of small sized flakes (typically <1 μm^2)[22] with a low exfoliation efficiency.[19]

In comparison, electrochemical exfoliation has emerged as a promising approach for producing high-quality graphene and other 2D materials with high efficiency and at low cost.[23−25] Inspired by the earlier research on graphene, electrochemical delamination of BP has been carried out in both aqueous[26] and N,N-dimethylformamide electrolytes.[27] In contrast to the oxidative anodic delamination,[26,28,29] cathodic exfoliation of BP in a nonaqueous system offers a better alternative for the isolation of high-quality nonoxidative FLBP. To date, there has been limited reports on the cathodic exfoliation of BP. The key impediment lies in identification of suitable intercalants for sufficient ion intercalations and efficient expansion toward a high production rate of thin flakes. To overcome this issue, we devise an ultrafast cathodic expansion technique of bulk BP using an organic electrolyte consisting of tetraalkylammonium (TAA) salts in aprotic polar solvents, which results in the production of high-quality FLBP with ultrahigh yield (>80%). Our results reveal that the exfoliation efficiency of BP is controlled not only by the cathodic potential but also by the size of the solvated TAA cations. By choosing an appropriate ammonium cation, bulk BP can be rapidly expanded in the organic electrolyte within several minutes and remained well-dispersed in an abundance of organic solvents without the need for prolonged ultrasonication. The resulting exfoliated FLBP flakes (average thickness ~5 layers) exhibit large lateral area (~10 μm^2 in average), ultralow defects, and high hole carrier mobilities (up to 100 $cm^2\ V^{-1}\ s^{-1}$ and 60 $cm^2\ V^{-1}\ s^{-1}$ on average). In addition, the fully expanded BP can be readily dispersed in low-boiling and environmentally benign solvents to form excellent inks for use in large-area inkjet printing of FLBP photodetectors.

RESULTS AND DISCUSSION

Compared to alkali cations such as Li and Na, organic TAA cations which possess a larger ionic diameter can be inserted into the interlayer space of layered materials along the *c*-axis direction to expand the lattice to a greater extent.[30] A judicious choice of solvent serves as another key factor for the cathodic exfoliation of BP. In our experiments, dimethyl sulfoxide (DMSO) was chosen as the organic electrolyte due to its high dispersion capability of BP[31] and strong donicity, which facilitates the formation of solvated cations for high intercalation efficiency.[32,33] Most importantly, we found that DMSO with a high boiling point can effectively protect as-exfoliated FLBP from being attacked by O_2 during air exposure.

With this in mind, we attempted the electrochemical exfoliation of bulk BP in an organic electrolyte containing TAA tetrafluoroborate salts and DMSO. To better understand the electrochemical charging process, we designed an electrochemical cell equipped with an optical microscope (as illustrated in Figure 1a) for the *in situ* visualization of the intercalation and expansion of a BP cathode in DMSO solution containing 0.001 M tetrabutylammonium tetrafluoroborate (TBAB) salts by performing cyclic voltammetry (CV)

DOI: 10.1021/acs.chemmater.8b00521
Chem. Mater. 2018, 30, 2742−2749

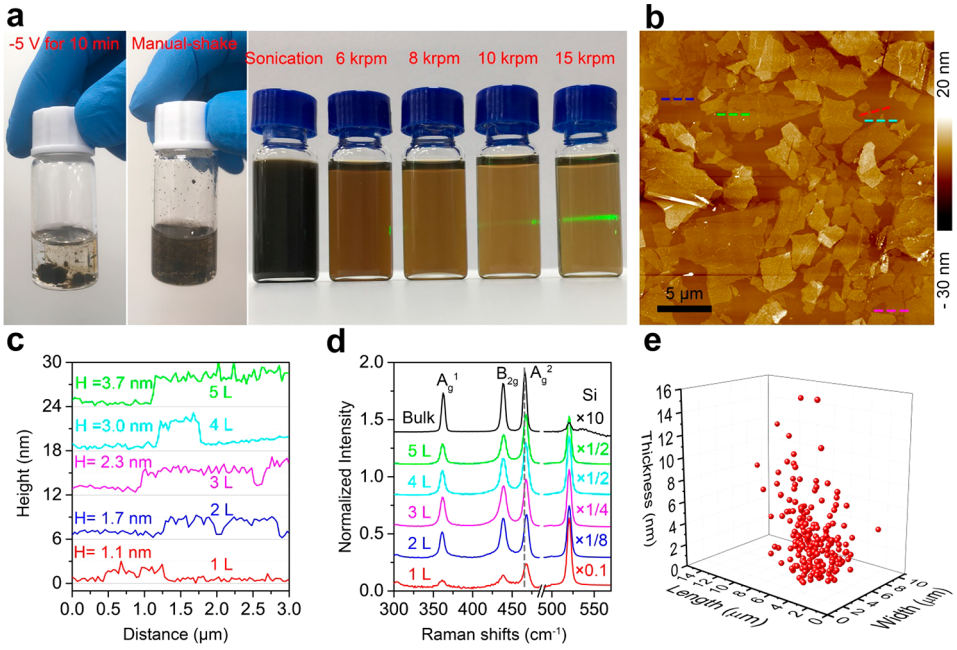

Figure 2. Basic characterization of as-exfoliated FLBP. (a) Photographs of (left) bulk BP in DMSO after electrochemical charging at −5 V for 10 min; (center) dispersion of expanded BP via manual-shaking; (right) FLBP dispersions centrifuged at different speeds exhibiting the Tyndall effect. (b) A representative AFM image of FLBP flakes deposited onto a SiO_2/Si substrate via drop-casting and annealed at 250 °C for 2 h in forming gas (H_2/Ar = 5/95). (c) AFM height profile and (d) Raman spectra of the exfoliated BP flakes with different thicknesses ranging from one to five layers. (e) The statistic information on the size (length and width) and thickness distribution of exfoliated FLBP flakes.

measurements. (Figure S4 and Supplementary Video 1) With the aid of the optical microscope, we observed that the bulk BP electrode remained unchanged in the high voltage range of U > − 3 V (as shown in the inset of Figure 1c, voltage is applied to the BP electrode in a two-electrode system with Pt wire as the counter electrode throughout this article unless otherwise stated) but underwent a slight volume expansion accompanied by the formation of tiny bumps on the surface of the electrode once the voltage was decreased to −3.5 V (inset of Figure 1d). In contrast, a dramatic volume expansion of BP occurred rapidly upon a decrease of the voltage to a more negative value of −5 V (inset of Figure 1e and Supplementary Video 1). *Ex situ* cross-sectional scanning electron microscopy (SEM) imaging was conducted to probe the morphological change of the BP electrode after the application of different cathodic potentials. Bulk BP exhibits the typical closely stacked lamellar structures before charging (Figure 1c), which evolves into accordion-like structures with the voids formed between layers (as marked by blue arrows in Figure 1d) as the charging voltage is decreased to −3.5 V. At a lower voltage of −5 V, a remarkable volume expansion of BP accompanied by edge roughening and wrinkling was observed by SEM imaging.

Our *in situ* optical microscopy and *ex situ* SEM characterization reveal two critical steps for the electrochemical charging and exfoliation of BP. These include the cointercalation of the solvated TAA complex into the interlayer space of bulk BP followed by the electrochemical decomposition of the intercalated compounds into gaseous species, creating the driving force for the ultrafast expansion of bulk BP. *In situ* CV measurements (Figure S4) reveal a pronounced cathodic peak around −3.5 V, which can be attributed to the intercalation of TAA cations into the interlayer space of BP. As the cathodic potential is further decreased below −4 V, the electrochemical decomposition of DMSO[34] and TAA ions[35] produces gaseous species such as dimethyl sulfite (Figure S3) and alkane,[35] resulting in the dramatic volume expansion of BP (Figure 1e). The decomposition of the intercalants is further supported by the experimental observation of tiny gas bubbles formed at the electrode at low reduction potential (Supplementary Video 2). In addition, our thermogravimetric analysis (TGA) reveals the presence of intercalated DMSO molecules in electrochemically expanded BP (refer to Figure S6 for details).

The ultrafast cathodic expansion of bulk BP described herein offers a facile and efficient exfoliation method of BP on a large scale. Upon the application of a reduction potential of −5 V, bulk BP undergoes rapid volume expansion by tens of times in a short time frame (tens of seconds) even in a dilute electrolyte solution consisting of 0.001 M TBA cations in DMSO (Supplementary Videos 2and 3). The fully expanded BP (Figure S7) was found to be readily dispersible in organic electrolytes to form a homogeneous dispersion up to ∼2 mg/mL with the mere aid of manual shaking or mild sonication (100 W for 1−3 min) as shown in Figure 2a. Typically, the flakes with large thickness or lateral size are prone to precipitate during centrifugation, which can be used to separate the thin flakes in the solutions from large and thick flakes in the sediment.[36,37] The centrifugation of initial BP dispersion at different speeds produces a series of solutions with different colors that also exhibit the characteristic Tyndall effect as shown in the right panel of Figure 2a. As the centrifugation speed is increased, the color of solution evolves from dark brown (2000 rmp) to yellow (15000 rmp), suggesting the presence of a significant amount of FLBP in all the dispersions. We also found that the yield of FLBP obtained was higher than 80% when TBA cations were used for electrochemical intercalation and expansion. In addition, we repeated the experiment using a series of TAA cations with different alkyl chains ranging from methyl to octyl groups to explore the relationship between the size of cations and exfoliation efficiency (refer to Figures S8 and S9). It is naturally expected

DOI: 10.1021/acs.chemmater.8b00521
Chem. Mater. 2018, 30, 2742−2749

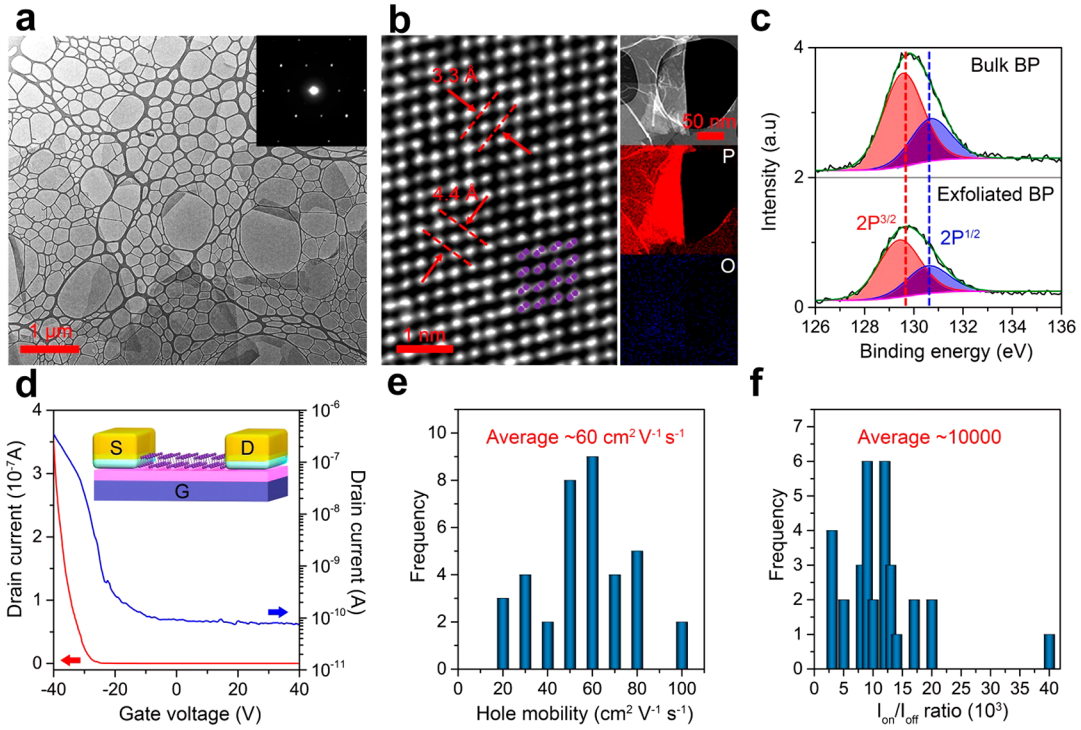

Figure 3. Structural characterization and charge transport measurement of the exfoliated FLBP and FET devices. (a) Large-scale TEM image of FLBP flakes with the corresponding SAED pattern (inset). (b) HR-TEM imaging resolves atomic lattice structures of FLBP (left). The atomic model structure of BP was superimposed in HR-TEM imaging. TEM-EELS imaging of exfoliated FLBP (right) by monitoring the signals associated with the $L_{2,3}$-edges of P (131 eV) and K-edge of O (532 eV). (c) P 2p core level XPS spectra of bulk BP and the exfoliated FLBP. (d) A representative charge transport curve for a FLBP FET device. The drain current is measured as a function of gate voltage on a linear scale (red, left) and a logarithmic scale (blue, right). A schematic illustration of an as-fabricated device is included in the inset of (d). (e and f) Histograms of the hole-mobility and on/off ratio for the FLBP FET devices.

that the energy barrier of the ion intercalation of BP at the initial charging stage is proportional to the alkyl chain length of TAA cations. However, among all the cations investigated, TBA exhibited the greatest exfoliation efficiency in terms of expansion rate (in minutes) and yield of FLBP (>80%). In contrast, the smallest tetramethylammonium (TMA) and largest tetraoctylammonium (TOA) cations demonstrate negligible exfoliation effect. These observations suggest that the size of solvated cations rather than the TAA cation alone plays a key role in determining the efficiency of intercalation and exfoliation of BP. To further prove this, we performed molecular dynamic simulation to understand the interplay between alkyl chain length and the size of solvation shell in the DMSO electrolyte (Figures S10 and S11). In general, as the alkyl chain length increases from the methyl to octyl group, the number of DMSO molecules in the first solvation shell decreases, though there is a slight increase from propyl to butyl (Figure S11). This suggests that as the alkyl chain length increases, there is less space accessible to the DMSO molecules in the first solvation shell due to repulsions from the alkyl chains. During the intercalation process, DMSO molecules in the closest solvation shell migrate along with the TAA cations under external electric field. The smallest TMA cations are surrounded by the largest number of DMSO molecules to form a large solvation shell, presumably resulting in a high intercalation barrier and thus poor exfoliation efficiency. On the other hand, although the solvated TOA complex contains few solvent molecules, its own bulky structure similarly results in poor intercalation and hence exfoliation efficiency. In contrast, the size of the solvated TBA complex is comparable to the van der Waal diameter of the TBA cation. Furthermore, the flexibility of the butyl group enables a flattened TBA cation to reduce its vertical dimension to 0.47 nm, resulting in a more efficient intercalation.[35]

In the following discussion, we will focus on the characterization of FLBP thin flakes exfoliated using TBA intercalants due to their excellent intercalation and expansion efficiency. The FLBP dispersion obtained after centrifuging the expanded BP solution at 2000 rpm for 10 min (~0.2 mg mL^{-1}) will be used to assess the flake morphologies as described below. The morphology of exfoliated BP flakes was first examined using an optical microscope and an atomic force microscope (AFM). The dark blue and purple optical contrast of BP flakes dispersed on a SiO_2/Si substrate suggests that the majority of flakes synthesized here are few-layer BP flakes[38] (Figure S13). The apparent AFM height of several representative microsized FLBP was determined to be 1.1 nm, 1.7 nm, 2.3 nm, 3.0 nm, and 3.7 nm, which can be assigned to monolayer, bilayers, trilayers, tetralayers, and pentalayers of BP, respectively (Figure 2c). In this regard, it should be noted that the apparent height measured for monolayer BP (~1.1 nm) would generally be expected to increase with the roughness of the SiO_2 substrate or the presence of solvent residue.[26] We also performed Raman spectroscopic measurement on the as-imaged flakes to further assess their thickness and crystal quality. As shown in Figure 2d, the Raman spectra (532 nm laser) acquired at different BP flakes ranging from monolayer to bulk all exhibit three representative features centered at 361.2 cm^{-1}, 439.5 cm^{-1}, and 468.6 cm^{-1}, corresponding to the out-of-plane (A_g^1) and two in-plane (B_{2g} and A_g^2) phonon modes, respectively.[38,39] The

DOI: 10.1021/acs.chemmater.8b00521
Chem. Mater. 2018, 30, 2742−2749

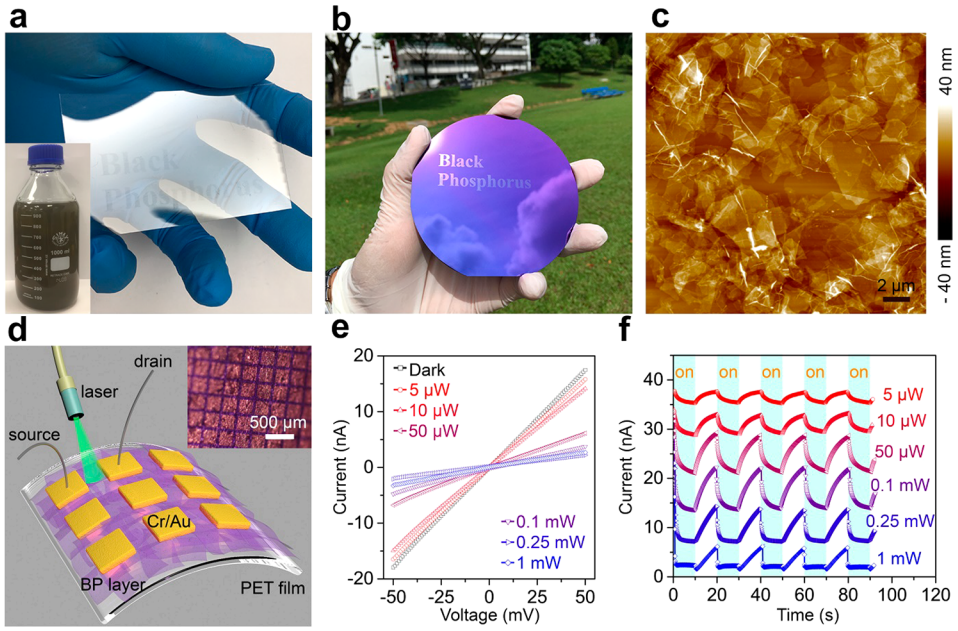

Figure 4. Inkjet printing of as-exfoliated FLBP flakes. (a,b) Inkjet printing of FLBP to form the patterns of "black phosphorus" on a (a) PET and a (b) 4-in. SiO_2/Si wafer. Inset of a: large-scale production of exfoliated FLBP dispersed in 1 L of DMSO solution (2 mg/mL). (c) AFM imaging of printed BP thin films on a SiO_2/Si substrate. (d) Schematic illustration and optical microscopic image (inset) of the large-area photodetector consisting of FLBP thin films deposited on a PET substrate. (e) *I*−*V* characteristics and the corresponding (f) photoresponse (at a bias of 0.05 V) of large-area FLBP optical devices under global irradiation of a 532 nm laser with different power levels.

presence of these lattice vibration modes suggests that the exfoliated BP flakes are highly crystalline. The intensity ratio of $I_{A_g^1}/I_{Si}$ was observed to increase as a function of flake thickness, consistent with the previous report on mechanically exfoliated FLBP.[17] The statistical analysis of the size (length and width) and thickness distribution of as-exfoliated FLBP was conducted by examining ∼300 flakes using AFM imaging. The histogram obtained (Figure 2e) reveals that the average size of the exfoliated few-layer BP is ∼10 μm^2, while the average thickness of the exfoliated BP flakes is around 4 nm, which is equivalent to 5 layers (Figure S14). Remarkably, the size of individual exfoliated FLBP flakes could reach tens of micrometers by reducing the sonication duration to tens of seconds or by replacing sonication with gentle manual shaking as shown in Figure S15.

We also performed intensive characterization of exfoliated FLBP to assess their crystallinity and chemical composition via a series of characterization techniques including high-resolution transmission electron microscopy (HR-TEM), electron energy loss spectroscopy (EELS), and X-ray photoelectron spectroscopy (XPS). Representative large-scale TEM imaging resolves several microsized FLBP flakes for further characterization (Figure 3a). Through selected area electron diffraction (SAED), we observed the characteristic orthorhombic crystal structure of the FLBP flakes (inset of Figure 3a), indicating a high crystallinity of the exfoliated BP thin films.[40] In addition, the atomic lattice of exfoliated FLBP was readily resolved via HR-TEM imaging as shown in Figure 3b. The lattice constants were determined to be 3.3 Å (along the zigzag direction) and ∼4.4 Å (along the armchair direction), in good agreement with previous reports.[6,31,40] In addition, TEM-EELS imaging was conducted to provide chemical analysis of FLBP by monitoring the signals associated with the $L_{2,3}$-edges of P (131 eV) and K-edge of O (532 eV). As shown in Figure 3b (right panel), the TEM-EELS mapping reveals a uniform distribution of phosphorus atoms over the entire exfoliated flake, while the absence of an oxygen-related signal proves that exfoliated FLBP underwent little or no oxidation.[18] The production of nonoxidative FLBP via the method developed here was further supported by the XPS elemental analysis of exfoliated BP flakes. Figure 3c shows the P 2p core-level XPS spectra acquired on the exfoliated FLBP (lower panel) and on pristine bulk BP crystal (upper panel). The XPS results reveal that both pristine BP (*in situ* exfoliated) and electrochemically exfoliated BP give rise to only the characteristic P 2p doublet peaked at 129.7 and 130.6 eV corresponding to the P $2p_{3/2}$ and P $2p_{1/2}$ components, respectively. The absence of a sub-band at ∼134 eV associated with oxidized phosphorus confirms that the FLBP synthesized here is free of oxidation.[41,42] It is well-known that the ambient degradation of mechanically exfoliated BP thin flakes occurs shortly after exfoliation, which greatly limits its potentials in applications. Interestingly, we found that electrochemically exfoliated FLBP dispersed in DMSO electrolyte displays a considerably enhanced air stability. The flakes coated on top of a SiO_2/Si wafer remain stable up to 10 h (>150 h) in ambient conditions with (without) light exposure, in sharp contrast to the rapid (∼1 h) degradation of MEBP flakes of similar thickness (Figure S16). The improved stability can be attributed to the formation of a solvation shell from the residual solvent molecules which act as a barrier to protect the BP surface from reacting with water or oxygen, consistent with a previous report.[41] Such protection is crucial for the large-scale production of BP thin flakes in ambient conditions for further processing and device fabrications.

The high crystallinity and excellent air stability of exfoliated FLBP imply its potential in charge transport applications. Hence, we fabricated a series of back-gated field effect transistor (FET) devices (>30 devices) to gain statistic information on the electrical properties of the as-prepared FLBP flakes. A typical FET device consists of individual microsized FLBP

DOI: 10.1021/acs.chemmater.8b00521
Chem. Mater. 2018, 30, 2742−2749

flakes placed onto a 300 nm SiO_2/Si substrate with top-contacted Cr (3 nm)/Au (50 nm) electrodes (as illustrated in the inset of Figure 3d). A representative charge transport curve (drain current as a function of gate voltage) of the individual FET devices is presented in Figure 3d. As shown in Figure 3e and f, FLBP FET devices exhibit a high mean hole mobility of ~60 $cm^2 V^{-1} s^{-1}$ (up to ~100 $cm^2 V^{-1} s^{-1}$) with a high on/off ratio (~1×10^4 in average), proving their superiority to the devices which use the BP thin flakes synthesized via other solution-phase exfoliation methods.[41,42] The excellent charge transport properties of exfoliated BP can be attributed to its low density of defects and low degree of surface oxidation, which arise as a result of the nonoxidative exfoliation of bulk BP without a need for prolonged agitation in our method.

Exfoliated FLBP not only exhibits excellent electronic properties but also high solution processability. It can be readily dispersed in a wide range of solvents including nonpolar and polar aprotic and protic solvents with the aid of gentle sonication (Figure S18). As-exfoliated BP also shows excellent dispersibility in solvents with low boiling points such as alcohol and water. This makes as-exfoliated FLBP particularly attractive for the preparation of functional inks for inkjet printing, which is a highly promising technique for large-scale and high speed device fabrication.[43,44] Alcohols are widely used as the solvent for preparing 2D material inks because their low surface tension favors substrate wetting, and their low boiling points allow for fast ink drying.[44] To our delight, the exfoliated BP thin layers can form stable concentrated dispersions (up to 2 mg/mL) in alcohol (e.g., IPA), which can be directly used as functional inks without introducing extra additives (inset of Figure 4a). Inkjet printing using BP inks was carried out with a 20 μm diameter printer nozzle to create the desired patterns on flexible substrates (e.g., PET) or on a SiO_2 wafer at large scale. As a proof-of-concept demonstration, we printed the word "black phosphorus" on both flexible PET and SiO_2 wafer substrates (Figure 4a,b). As revealed in the AFM image (Figure 4c and Figure S19), the excellent BP inks prepared here allow us to obtain continuous and uniform FLBP thin films printed on a wide range of substrates.

We also investigated the performance of inkjet-printed BP when integrated into optoelectronic devices. As shown in Figure 4d, we patterned Au electrode arrays on the printed BP films as a large-area photodetector. The electrical characteristics of the device were measured in dark and illuminated conditions. The illuminated experiments were carried out under global irradiation using a laser (λ = 532 nm, power from 0 to 1 mW, and spot size ~2 mm^2) with different light intensities. Remarkably, the $I-V$ curves measured on such a large-area device reveal an anomalous negative photoresponse, namely, a decrease in current upon the irradiation of a laser beam onto the device (Figure 4e). The generation of negative photoresponse (Figure 4e and f) of the large-area FLBP device can be ascribed to the following effects: (i) The intercalated TAA cations may act as acceptors and thus increase the hole concentration in FLBP, resulting in high conductivity in a dark environment. Upon illumination, a photoexcited TAA cation may undergo photodesorption or rearrangement of its adsorption geometry on BP. This could weaken the charge transfer between TAA cations and BP, leading to the decrease of carrier concentration and conductivity of BP. The molecular photodesorption effect has also been observed in carbon nanotube systems.[45] An increase of laser power is expected to produce a larger portion of photoexcited TAA cations inactive for p-doping, decreasing the photocurrent as shown in Figure 4e. (ii) A decrease of photocurrent upon irradiation can also be attributed to the trapping of holes due to the presence of the trap state or interlayer junctions of the vertically stacked FLBP. Such an effect can result in a reduction of total carrier concentration and photoconductivity upon light irradiation. A similar negative photoresponse has been reported in III–V semiconducting nanowires and large-area carbon nanotube devices.[46,47] With periodical light illumination and a fixed bias of 50 mV, the output current of the device as a function of time displays an obvious on and off behavior (Figure 4f). Photoresponsivity (R_{res}), one of the critical parameters of a photodetector, is calculated to be ~ −1.51 mA W^{-1} under 0.5 mW illumination. Accordingly, the external quantum efficiency, $EQE = (hcR_{res})/(e\lambda)$, is determined to be ~ −0.35%. Photodetectivity (D^*), on the other hand, is determined to be -1.18×10^8 Jones. These results demonstrate that exfoliated FLBP can be used to fabricate broad-band photonic devices at large-scale and low-cost.

CONCLUSION

In summary, we have devised a method for producing high-quality large-sized few-layer BP at high yield via ultrafast electrochemical cathodic expansion of BP. The yield of FLBP (>80%) obtained from bulk BP electrode is significantly higher than that produced by liquid-phase exfoliation methods. The FLBP via our method shows extraordinary crystal quality and electronic properties. In addition, fully expanded BP can be further dispersed in a wide range of solvents. BP thin flakes dispersed in high-boiling solvents exhibit high air stability, facilitating the development of long-term stable electronic and optoelectronic devices. Concentrated BP inks can also be obtained using low-boiling point solvents, which make them suitable for use in large-area inkjet printing technology to produce uniform BP thin films for printable optoelectronic devices. Therefore, the high quality and solution processable FLBP obtained here holds great promise for use in a wide range of applications ranging from hybrid compositions and wearable sensors to printable electronic and photonics devices.

METHODS

Electrochemical Expansion of Bulk BP. Electrochemical intercalation and expansion of bulk BP. The electrochemical expansion of bulk BP was performed using an electrochemical workstation (CHI 760E) consisting of a two-electrode system. Bulk BP (HQ graphene, purity 99.9%, Figure S1a) was placed as the working cathode, and a Pt wire was used as the counter electrode. For sample preparation in large quantities, the experiment was carried out in a 30 mL beaker (Figure S1c). A nonaqueous solution consisting of 0.01 M TAA and DMSO was used as electrolyte. The ultrafast expansion of bulk BP can be achieved once a cathodic voltage lower than −5 V is applied (refer to Supplementary Video 3). The expanded BP flakes can be further exfoliated and dispersed in designated solvents via manual shaking or gentle sonication at low power for 1–3 min. All the solvents and ammonium ions were sourced from Sigma-Aldrich (>99% of purity) and used as received. Electrochemical exfoliation of bulk BP was carried out in ambient conditions (the as-received bulk BP sample was stored in the glovebox). Sample preparation for Raman and AFM characterization was also carried out in ambient conditions.

Characterization. Optical imaging of exfoliated BP flakes on the SiO_2/Si substrate was conducted using an Olympus BX51 microscope. The morphology and thickness of FLBP flakes were characterized by SEM (FEI Verios 460 operated at 2 kV and 100 pA), AFM (Bruker Multimode 8 and DIMENSION FastScan), and HRTEM (FEI Titan 80–300 S/TEM operated at 200 kV). In addition, we also carried out

DOI: 10.1021/acs.chemmater.8b00521
Chem. Mater. 2018, 30, 2742–2749

thermogravimetric analysis (TGA) of exfoliated BP flakes up to 600 °C to evaluate compositional information (Discovery TGA Thermogravimetric Analyzer, TA Instruments, with a heating rate of 5 °C min^{-1} in nitrogen atmosphere). The electrolyte was analyzed by gas chromatography−mass spectrometry (GC-MS, Agilent HP6890 DC with HP 5973 Mass Selective detector) to reveal the electrochemical process. Raman spectroscopic measurements of exfoliated BP (WITec Alpha 300R) were performed at room temperature with laser excitation at 532 nm. XPS (Omicron EAC2000-125) elemental analysis of exfoliated BP was conducted using Al Kα radiation ($h\nu$ = 1486.6 eV).

Photocurrent Measurements. The photoresponse of an FLBP-based photodetector was carried out by measuring the typical characteristics of FLBP devices under irradiation of a continuous wave laser beam from diode lasers (532 nm). The applied bias and the output current were provided and collected via a Keithley 6430 source meter.

■ ASSOCIATED CONTENT

Supporting Information

The Supporting Information is available free of charge on the ACS Publications website at DOI: 10.1021/acs.chemmater.8b00521.

Detailed experimental procedures, characterization, and calculation (PDF)

Video 1-In situ CV and optical microscope video (AVI)

Video 2-Expansion video of bulk BP in 0.001 M TBAB at -5 V (AVI)

Video 3-Expansion video of bulk BP in 0.01 M TBAB at -5 V (AVI)

■ AUTHOR INFORMATION

Corresponding Authors

*(C.S.) E-mail: chmsuc@szu.edu.cn.

*(J.L.) E-mail: chmluj@nus.edu.sg.

ORCID

Jing Li: 0000-0002-2159-1650

Chenliang Su: 0000-0002-8453-1938

Jiong Lu: 0000-0002-3690-8235

Author Contributions

¶J. Li and C.C. contributed equally to this work.

Notes

The authors declare no competing financial interest.

■ ACKNOWLEDGMENTS

J. Lu acknowledges the financial support from NUS start-up grant (R-143-000-621-133), Tier 1 (R-143-000-637-112), and MOE Tier 2 grant (R-143-000-682-112). J. Li acknowledges the financial support from the National Natural Science Foundation of China (21703143). C.L.S. acknowledges the support from Shenzhen Peacock Plan (Grant No. 827-000113, KQTD2016053112042971) and the Educational Commission of Guangdong Province (2016KCXTD006 and 2016KSTCX126).

■ REFERENCES

(1) Liu, H.; Neal, A. T.; Zhu, Z.; Luo, Z.; Xu, X.; Tománek, D.; Ye, P. D. Phosphorene: An Unexplored 2D Semiconductor with a High Hole Mobility. *ACS Nano* **2014**, *8*, 4033−4041.

(2) Li, L.; Yu, Y.; Ye, G. J.; Ge, Q.; Ou, X.; Wu, H.; Feng, D.; Chen, X. H.; Zhang, Y. Black phosphorus field-effect transistors. *Nat. Nanotechnol.* **2014**, *9*, 372−377.

(3) Yuan, H.; Liu, X.; Afshinmanesh, F.; Li, W.; Xu, G.; Sun, J.; Lian, B.; Curto, A. G.; Ye, G.; Hikita, Y. Polarization-sensitive broadband photodetector using a black phosphorus vertical p−n junction. *Nat. Nanotechnol.* **2015**, *10*, 707.

(4) Xia, F.; Wang, H.; Jia, Y. Rediscovering black phosphorus as an anisotropic layered material for optoelectronics and electronics. *Nat. Commun.* **2014**, *5*, 4458.

(5) Lu, J.; Yang, J.; Carvalho, A.; Liu, H.; Lu, Y.; Sow, C. H. Light−Matter Interactions in Phosphorene. *Acc. Chem. Res.* **2016**, *49*, 1806−1815.

(6) Sun, J.; Lee, H.-W.; Pasta, M.; Yuan, H.; Zheng, G.; Sun, Y.; Li, Y.; Cui, Y. A phosphorene−graphene hybrid material as a high-capacity anode for sodium-ion batteries. *Nat. Nanotechnol.* **2015**, *10*, 980.

(7) Batmunkh, M.; Bat-Erdene, M.; Shapter, J. G. Phosphorene and Phosphorene-Based Materials − Prospects for Future Applications. *Adv. Mater.* **2016**, *28*, 8586−8617.

(8) Ge, S.; Li, C.; Zhang, Z.; Zhang, C.; Zhang, Y.; Qiu, J.; Wang, Q.; Liu, J.; Jia, S.; Feng, J.; Sun, D. Dynamical Evolution of Anisotropic Response in Black Phosphorus under Ultrafast Photoexcitation. *Nano Lett.* **2015**, *15*, 4650−4656.

(9) Tran, V.; Soklaski, R.; Liang, Y.; Yang, L. Layer-controlled band gap and anisotropic excitons in few-layer black phosphorus. *Phys. Rev. B: Condens. Matter Mater. Phys.* **2014**, *89*, 235319.

(10) Castellanos-Gomez, A. Black Phosphorus: Narrow Gap, Wide Applications. *J. Phys. Chem. Lett.* **2015**, *6*, 4280−4291.

(11) Kou, L.; Chen, C.; Smith, S. C. Phosphorene: Fabrication, Properties, and Applications. *J. Phys. Chem. Lett.* **2015**, *6*, 2794−2805.

(12) Liu, H.; Du, Y.; Deng, Y.; Ye, P. D. Semiconducting black phosphorus: synthesis, transport properties and electronic applications. *Chem. Soc. Rev.* **2015**, *44*, 2732−2743.

(13) Chen, C.; Youngblood, N.; Peng, R.; Yoo, D.; Mohr, D. A.; Johnson, T. W.; Oh, S.-H.; Li, M. Three-Dimensional Integration of Black Phosphorus Photodetector with Silicon Photonics and Nanoplasmonics. *Nano Lett.* **2017**, *17*, 985−991.

(14) Wang, K.; Szydłowska, B. M.; Wang, G.; Zhang, X.; Wang, J. J.; Magan, J. J.; Zhang, L.; Coleman, J. N.; Wang, J.; Blau, W. J. Ultrafast Nonlinear Excitation Dynamics of Black Phosphorus Nanosheets from Visible to Mid-Infrared. *ACS Nano* **2016**, *10*, 6923−6932.

(15) Hao, C.; Wen, F.; Xiang, J.; Yuan, S.; Yang, B.; Li, L.; Wang, W.; Zeng, Z.; Wang, L.; Liu, Z.; Tian, Y. Liquid-Exfoliated Black Phosphorous Nanosheet Thin Films for Flexible Resistive Random Access Memory Applications. *Adv. Funct. Mater.* **2016**, *26*, 2016−2024.

(16) Novoselov, K. S.; Falko, V. I.; Colombo, L.; Gellert, P. R.; Schwab, M. G.; Kim, K. A roadmap for graphene. *Nature* **2012**, *490*, 192−200.

(17) Favron, A.; Gaufres, E.; Fossard, F.; Phaneuf-Lheureux, A.-L.; Tang, N. Y. W.; Levesque, P. L.; Loiseau, A.; Leonelli, R.; Francoeur, S.; Martel, R. Photooxidation and quantum confinement effects in exfoliated black phosphorus. *Nat. Mater.* **2015**, *14*, 826−832.

(18) Huang, Y.; Qiao, J.; He, K.; Bliznakov, S.; Sutter, E.; Chen, X.; Luo, D.; Meng, F.; Su, D.; Decker, J.; Ji, W.; Ruoff, R. S.; Sutter, P. Interaction of Black Phosphorus with Oxygen and Water. *Chem. Mater.* **2016**, *28*, 8330−8339.

(19) Dhanabalan, S. C.; Ponraj, J. S.; Guo, Z.; Li, S.; Bao, Q.; Zhang, H. Emerging Trends in Phosphorene Fabrication towards Next Generation Devices. *Adv. Sci.* **2017**, *4*, 1600305.

(20) Woomer, A. H.; Farnsworth, T. W.; Hu, J.; Wells, R. A.; Donley, C. L.; Warren, S. C. Phosphorene: Synthesis, Scale-Up, and Quantitative Optical Spectroscopy. *ACS Nano* **2015**, *9*, 8869−8884.

(21) Chen, L.; Zhou, G.; Liu, Z.; Ma, X.; Chen, J.; Zhang, Z.; Ma, X.; Li, F.; Cheng, H.-M.; Ren, W. Scalable Clean Exfoliation of High-Quality Few-Layer Black Phosphorus for a Flexible Lithium Ion Battery. *Adv. Mater.* **2016**, *28*, 510−517.

(22) Hanlon, D.; Backes, C.; Doherty, E.; Cucinotta, C. S.; Berner, N. C.; Boland, C.; Lee, K.; Harvey, A.; Lynch, P.; Gholamvand, Z.; Zhang, S.; Wang, K.; Moynihan, G.; Pokle, A.; Ramasse, Q. M.; McEvoy, N.; Blau, W. J.; Wang, J.; Abellan, G.; Hauke, F.; Hirsch, A.; Sanvito, S.; O'Regan, D. D.; Duesberg, G. S.; Nicolosi, V.; Coleman, J. N. Liquid

DOI: 10.1021/acs.chemmater.8b00521
Chem. Mater. 2018, 30, 2742−2749

exfoliation of solvent-stabilized few-layer black phosphorus for applications beyond electronics. *Nat. Commun.* **2015**, *6*, 8563.
(23) Lu, J.; Yang, J.-x.; Wang, J.; Lim, A.; Wang, S.; Loh, K. P. One-Pot Synthesis of Fluorescent Carbon Nanoribbons, Nanoparticles, and Graphene by the Exfoliation of Graphite in Ionic Liquids. *ACS Nano* **2009**, *3*, 2367−2375.
(24) Parvez, K.; Wu, Z.-S.; Li, R.; Liu, X.; Graf, R.; Feng, X.; Müllen, K. Exfoliation of Graphite into Graphene in Aqueous Solutions of Inorganic Salts. *J. Am. Chem. Soc.* **2014**, *136*, 6083−6091.
(25) Abdelkader, A. M.; Cooper, A. J.; Dryfe, R. A. W.; Kinloch, I. A. How to get between the sheets: a review of recent works on the electrochemical exfoliation of graphene materials from bulk graphite. *Nanoscale* **2015**, *7*, 6944−6956.
(26) Erande, M. B.; Pawar, M. S.; Late, D. J. Humidity Sensing and Photodetection Behavior of Electrochemically Exfoliated Atomically Thin-Layered Black Phosphorus Nanosheets. *ACS Appl. Mater. Interfaces* **2016**, *8*, 11548−11556.
(27) Huang, Z.; Hou, H.; Zhang, Y.; Wang, C.; Qiu, X.; Ji, X. Layer-Tunable Phosphorene Modulated by the Cation Insertion Rate as a Sodium-Storage Anode. *Adv. Mater.* **2017**, *29*, 1702372.
(28) Ambrosi, A.; Sofer, Z.; Pumera, M. Electrochemical Exfoliation of Layered Black Phosphorus into Phosphorene. *Angew. Chem., Int. Ed.* **2017**, *56*, 10443−10445.
(29) Zheng, J.; Tang, X.; Yang, Z.; Liang, Z.; Chen, Y.; Wang, K.; Song, Y.; Zhang, Y.; Ji, J.; Liu, Y.; Fan, D.; Zhang, H. Few-Layer Phosphorene-Decorated Microfiber for All-Optical Thresholding and Optical Modulation. *Adv. Opt. Mater.* **2017**, *5*, 1700026.
(30) Wang, J.; Manga, K. K.; Bao, Q.; Loh, K. P. High-Yield Synthesis of Few-Layer Graphene Flakes through Electrochemical Expansion of Graphite in Propylene Carbonate Electrolyte. *J. Am. Chem. Soc.* **2011**, *133*, 8888−8891.
(31) Yasaei, P.; Kumar, B.; Foroozan, T.; Wang, C.; Asadi, M.; Tuschel, D.; Indacochea, J. E.; Klie, R. F.; Salehi-Khojin, A. High-Quality Black Phosphorus Atomic Layers by Liquid-Phase Exfoliation. *Adv. Mater.* **2015**, *27*, 1887−1892.
(32) Govinda, V.; Attri, P.; Venkatesu, P.; Venkateswarlu, P. Temperature effect on the molecular interactions between two ammonium ionic liquids and dimethylsulfoxide. *J. Mol. Liq.* **2011**, *164*, 218−225.
(33) Govinda, V.; Attri, P.; Venkatesu, P.; Venkateswarlu, P. Evaluation of Thermophysical Properties of Ionic Liquids with Polar Solvent: A Comparable Study of Two Families of Ionic Liquids with Various Ions. *J. Phys. Chem. B* **2013**, *117*, 12535−12548.
(34) Luca, O. R.; Gustafson, J. L.; Maddox, S. M.; Fenwick, A. Q.; Smith, D. C. Catalysis by electrons and holes: formal potential scales and preparative organic electrochemistry. *Org. Chem. Front.* **2015**, *2*, 823−848.
(35) Zhong, Y. L.; Swager, T. M. Enhanced Electrochemical Expansion of Graphite for in Situ Electrochemical Functionalization. *J. Am. Chem. Soc.* **2012**, *134*, 17896−17899.
(36) Nicolosi, V.; Chhowalla, M.; Kanatzidis, M. G.; Strano, M. S.; Coleman, J. N. Liquid Exfoliation of Layered Materials. *Science* **2013**, *340*, 1226419.
(37) Ciesielski, A.; Samori, P. Graphene via sonication assisted liquid-phase exfoliation. *Chem. Soc. Rev.* **2014**, *43*, 381−398.
(38) Ling, X.; Liang, L.; Huang, S.; Puretzky, A. A.; Geohegan, D. B.; Sumpter, B. G.; Kong, J.; Meunier, V.; Dresselhaus, M. S. Low-Frequency Interlayer Breathing Modes in Few-Layer Black Phosphorus. *Nano Lett.* **2015**, *15*, 4080−4088.
(39) Ribeiro, H. B.; Pimenta, M. A.; de Matos, C. J. S.; Moreira, R. L.; Rodin, A. S.; Zapata, J. D.; de Souza, E. A. T.; Castro Neto, A. H. Unusual Angular Dependence of the Raman Response in Black Phosphorus. *ACS Nano* **2015**, *9*, 4270−4276.
(40) Castellanos-Gomez, A.; Vicarelli, L.; Prada, E.; Island, J. O.; Narasimha-Acharya, K. L.; Blanter, S. I.; Groenendijk, D. J.; Buscema, M.; Steele, G. A.; Alvarez, J. V.; Zandbergen, H. W.; Palacios, J. J.; van der Zant, H. S. J. Isolation and characterization of few-layer black phosphorus. *2D Mater.* **2014**, *1*, 025001.
(41) Kang, J.; Wood, J. D.; Wells, S. A.; Lee, J.-H.; Liu, X.; Chen, K.-S.; Hersam, M. C. Solvent Exfoliation of Electronic-Grade, Two-Dimensional Black Phosphorus. *ACS Nano* **2015**, *9*, 3596−3604.
(42) Wood, J. D.; Wells, S. A.; Jariwala, D.; Chen, K.-S.; Cho, E.; Sangwan, V. K.; Liu, X.; Lauhon, L. J.; Marks, T. J.; Hersam, M. C. Effective Passivation of Exfoliated Black Phosphorus Transistors against Ambient Degradation. *Nano Lett.* **2014**, *14*, 6964−6970.
(43) Hu, G.; Albrow-Owen, T.; Jin, X.; Ali, A.; Hu, Y.; Howe, R. C. T.; Shehzad, K.; Yang, Z.; Zhu, X.; Woodward, R. I.; Wu, T.-C.; Jussila, H.; Wu, J.-B.; Peng, P.; Tan, P.-H.; Sun, Z.; Kelleher, E. J. R.; Zhang, M.; Xu, Y.; Hasan, T. Black phosphorus ink formulation for inkjet printing of optoelectronics and photonics. *Nat. Commun.* **2017**, *8*, 278.
(44) Kelly, A. G.; Hallam, T.; Backes, C.; Harvey, A.; Esmaeily, A. S.; Godwin, I.; Coelho, J.; Nicolosi, V.; Lauth, J.; Kulkarni, A.; Kinge, S.; Siebbeles, L. D. A.; Duesberg, G. S.; Coleman, J. N. All-printed thin-film transistors from networks of liquid-exfoliated nanosheets. *Science* **2017**, *356*, 69−73.
(45) Chen, R. J.; Franklin, N. R.; Kong, J.; Cao, J.; Tombler, T. W.; Zhang, Y.; Dai, H. Molecular photodesorption from single-walled carbon nanotubes. *Appl. Phys. Lett.* **2001**, *79*, 2258−2260.
(46) Guo, N.; Hu, W.; Liao, L.; Yip, S.; Ho, J. C.; Miao, J.; Zhang, Z.; Zou, J.; Jiang, T.; Wu, S.; Chen, X.; Lu, W. Anomalous and Highly Efficient InAs Nanowire Phototransistors Based on Majority Carrier Transport at Room Temperature. *Adv. Mater.* **2014**, *26*, 8203−8209.
(47) Yang, Y.; Peng, X.; Kim, H.-S.; Kim, T.; Jeon, S.; Kang, H. K.; Choi, W.; Song, J.; Doh, Y.-J.; Yu, D. Hot Carrier Trapping Induced Negative Photoconductance in InAs Nanowires toward Novel Nonvolatile Memory. *Nano Lett.* **2015**, *15*, 5875−5882.

DOI: 10.1021/acs.chemmater.8b00521
Chem. Mater. 2018, 30, 2742−2749